## Faceting and step flow growth in the homoepitaxy of $Ga_2O_3$

**PIs** Martin Albrecht (C1.4), Günter Wagner (C3.5), Claudia Draxl and Matthias Scheffler (C2.1), Oliver Bierwagen (C3.3), Zbigniew Galazka (C3.1)

**Research team** Robert Schewski, Charlotte Wouters, Michele Baldini, Konstantin Lion, Patrick Vogt, Piero Mazzolini

**Participating Groups:** Paul-Drude-Institut für Festkörperelektronik, Leibniz-Institut für Kristallzüchtung, Humboldt-Universität zu Berlin (Festkörpertheorie), Fritz-Haber-Institut

An important advantage of $\beta$-$Ga_2O_3$ in contrast to other wide band gap semiconductors (e.g. SiC and GaN) is the availability of bulk single crystals that can be grown with high structural perfection from the melt.[1,2,3] Homoepitaxial growth is therefore the natural choice. In the last years impressive results on homoepitaxial growth have been obtained by different growth techniques (e.g. Metalorganic chemical vapor deposition (MOVPE),[4,5,6] molecular beam epitaxy (MBE)[7,8,9] and halide vapor phase epitaxy (HVPE)[10,11] on a variety of possible substrate orientations (among them (100), (010), (001), ($\bar{2}$01)). The substrate orientation has been chosen for pragmatic reasons, i.e. considering the achievable growth rates for the respective growth method and the available substrate size or a combination of them. Commercially available wafer sizes today range from 2 inch for ($\bar{2}$01) and (001) orientations (Novel Crystal technology) over 1 inch for (010) (Kyma Technologies) to sizes of 10x15 $mm^2$ and 10 x 10 $mm^2$ available for all other orientations. In MBE the growth rate on (010) is reportedly an order of magnitude higher than that on (100) substrates[9] while it is widely independent on substrate orientation in MOCVD.[6] An aspect that has been drawn little attention up to know is how the growth mode is influenced by the substrate orientation and growth conditions. The step flow growth mode, highly desirable to achieve homogeneous incorporation of dopants and atomically abrupt interfaces of heterostructures, e.g. in field effect transistors, has up to now exclusively been observed on the (100) surface for MBE[7,8] and MOCVD[12], while all other orientations resulted in faceted or macroscopically rough surfaces.[13,14,15,5]

In the framework of GraFOx we performed a focused study on the influence of surface orientations on the growth mode, in particular looking at surface faceting. To this end, we have combined the activities on bulk crystal growth, molecular beam epitaxy, metalorganic vapor phase epitaxy, electrical and structural characterization and theory.

### Surface energies

Up to now there is only a single work in literature that focuses on the structure and energetics of surfaces of $\beta$-$Ga_2O_3$ by DFT calculations.[16] Bermudez calculated the physical and electronic structure of the (100), (010), (001) and $(10\bar{1})$ facets. He showed that the nonpolar cleavage planes of $Ga_2O_3$, i.e. (100) and (001) have two possible terminations which are named A and B, while (010) surfaces have only one possible termination. The A termination of the (100) surface exhibits undersaturated O(II) and Ga (II) bonds, while the B surface consists of fully coordinated Ga(I) and O (I) atoms. In case of (001) both A and B surfaces contain unsaturated Ga atoms. The theoretical results of Bermudez confirmed common reasoning, i.e. that the cleavage planes had the lowest surface energies, with the (100) having the lowest energy followed by the c-plane and the (010) and (10-1) surface.

In our calculations we focused on a number of surfaces that have been experimentally observed but were not considered in theory so far. The focus was on the structure and structural relaxation of stoichiometric surfaces. For these surfaces the surface energy is independent of the individual chemical potentials under the conditions that bulk β-Ga$_2$O$_3$ is thermodynamically stable. Defects, adsorption processes or possible surface reconstructions were neglected. Figure 1(a) shows the calculated surface energies and those from previous calculations by Bermudez for comparison, where available. The energy of the surface slab is defined as

$$\gamma = \frac{1}{2A}(E_{slab} - Ne_{bulk})$$

Here, A is the surface area, $E_{slab}$ is the total energy of the slab supercell, $e_{bulk}$ is the total energy of the bulk cell per atom, and N is the number of atoms in the surface slab. The factor $\frac{1}{2}$ accounts for the two identical surfaces in the slab. HSE06 and PBEsol have been used for calculations. The results on surface energies, however, show little dependence on the employed exchange-correlation functional. $E_{slab}$ was calculated for the relaxed as well as the unrelaxed structures. Our calculations show two main results. First, in all cases, the surface energy is lowered substantially upon fully relaxing the surface slabs. This reduction, however, differs significantly between the different surfaces and may even change the order of their surface energies. While the surface energy of the (100)-B surface is only reduced by 0.2 J/m$^2$ (32% reduction in energy), the biggest reduction can be found for the ($\bar{2}$01)-A surface with 1.4 J/m2 (257%). Side views of both surfaces are shown in Figs. 6(b) and 6(c), respectively. The relaxation of the ($\bar{2}$01)-A surface is complex and leads to a significant flattening of the surface. The second important result is the finding that the ($\bar{2}$01)-A surface has the lowest energy after the (100)-B. This contradicts common assumptions assuming the cleavage planes to have the lowest energy. As we will see below, this finding can explain unexpected growth behaviour on the most stable (100) surface.
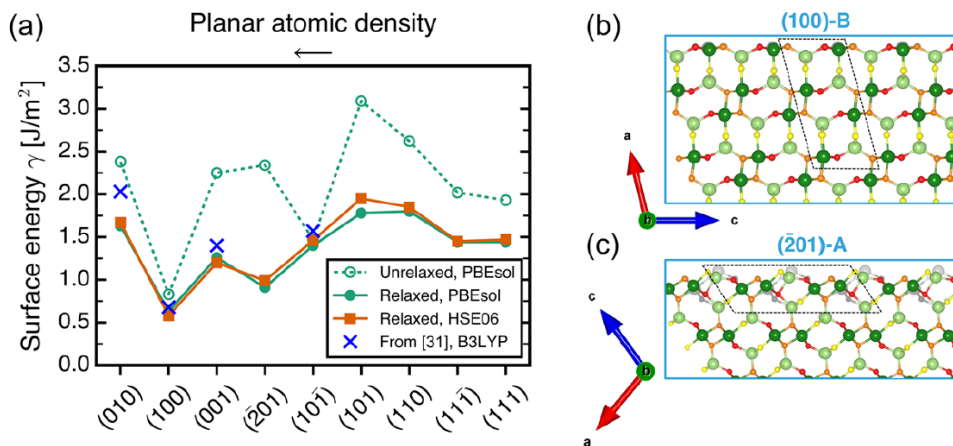


**Figure 1**. (a) Calculated energies of different β-Ga$_2$O$_3$ surfaces. The surface terminations are ordered from left to right on the x-axis according to decreasing planar atomic density. If more than one surface termination is available for a given Miller plane, only the termination with the lowest surface energy is shown. [(b) and (c)] Side view of the two surface terminations with the lowest surface energies. Two terminations (A and B) can be found for both the (100) and the ($\bar{2}$01) surfaces. Here, we only show the most stable termination for both Miller planes. The relaxed slab (colored spheres) is superimposed with the unrelaxed slab (light gray spheres). The dashed parallelograms indicate the surface unit cell.

**Faceting**

It is well known that faceting of crystalline material is driven by surface energy minimization but it is also influenced by kinetics. Growth and etching are not necessarily reciprocal as has been shown in early work by Wulff.[17] To unveil the driving force for faceting on $Ga_2O_3$ surfaces, detailed experimental studies have been performed *ex-situ* and *in-situ* on various substrate surfaces by the group at PDI. Experiments were done both, during epitaxial growth and during etching and oxygen plasma treatment in the MBE chamber changing T (surface mobility of adatoms) and the chemical potential (Ga vs. oxygen rich conditions). Ga-etching and high temperature annealing under oxygen has been performed for the (100), (010), ($\bar{2}$01) and the (001) surface. All surfaces are stable under oxygen plasma annealing. (100), (001) and ($\bar{2}$01) surfaces show well organized surface steps after oxygen annealing that correspond to the assigned miscut. The RHEED experiments prove that the (100) surface does not exhibit surface reconstruction in agreement with previous experimental and theoretical work, while indications for a surface reconstruction where found on the (001) plane under oxygen rich conditions. The (100) surface is the only one that is stable under Ga etching while (010) and (001) surfaces tend to form facets: the (010) surfaces split into (110) and (1-10) facets, aligned along [001] directions, while ($\bar{2}$01) and (101) facets aligned along [010] are present at (001) surfaces.

These results on faceting during Ga-etching agree well with faceting observed in epitaxial growth experiments on (010) surfaces, which indicate formation of {110} facets for layers grown on (010) substrates by MOCVD[6] and MBE.[18] Note that this holds for MOCVD despite of the fact that the layers were not Ga-etched before growth, i.e. growth experiments started with a flat surface. Growth on (001) oriented surfaces by Rafique et al.[15] and Han et al.[14] show facets aligned along [010] directions. Though no facets have been assigned by these authors, at least the alignment is consistent with those observed by our etching experiments showing ($\bar{2}$01) and (101) facets.

Considering faceting to be controlled by minimization of surface energies, i.e. by thermodynamics, our experiments are consistent with theory for (100) and (001) surfaces. In the first case, (001) surfaces exhibit the lowest surface energy and any formation of facets would increase it. In case of the (001) plane our calculations showed that ($\bar{2}$01) facets have the lower surface energy than (001). Our experimental observations suggest that the (110) and ($\bar{1}$10) β-$Ga_2O_3$ surfaces are thermodynamically more stable with respect to the (010) surface under metal-rich/oxygen poor (i.e., reducing) conditions. Though this is at conflict theory of stoichiometric surfaces (cf. Fig. 1) where {110} surfaces are energetically degenerate with (010), STEM studies of faceted (010) surfaces grown with In as a catalyst evidence the presence of nonstoichiometric {110} surfaces. As can be seen in Fig. 3b, the structure is not in accordance with the structure shown in Fig. 2(e). According to STEM, we observe exclusively tetrahedrally coordinated Ga atoms at the surface. The surface thus does not contain octahedrally coordinated Ga and fourfold coordinated oxygen atoms. However, a detailed analysis requires more experimental and theoretical work on pure (110) surfaces.
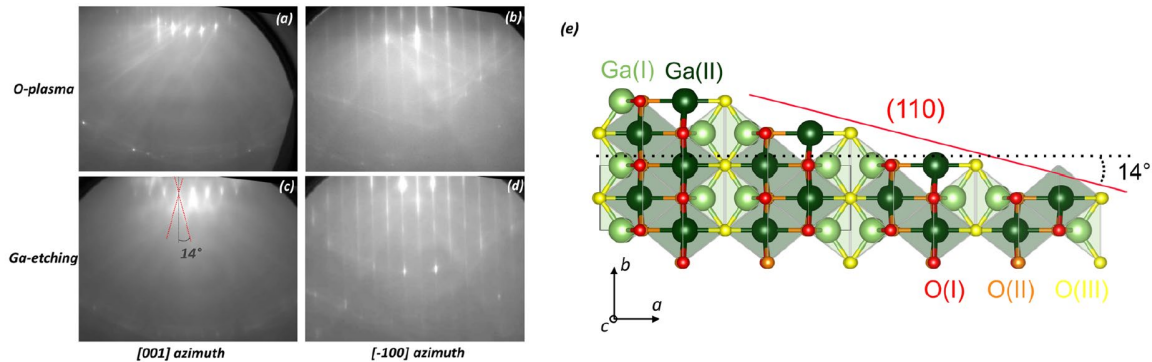
**FIG. 2**. RHEED patterns of O-plasma treated [(a) and (b)] and Ga-etched [(c) and (d)] β-Ga2O3 (010) substrates taken along [001] and [-100] azimuthal directions [(a),(c) and (b),(d), respectively]. The red dotted lines reported in (c) are a guide for the eye to highlight the presence of wedges. (e) β-Ga2O3 atomic model.
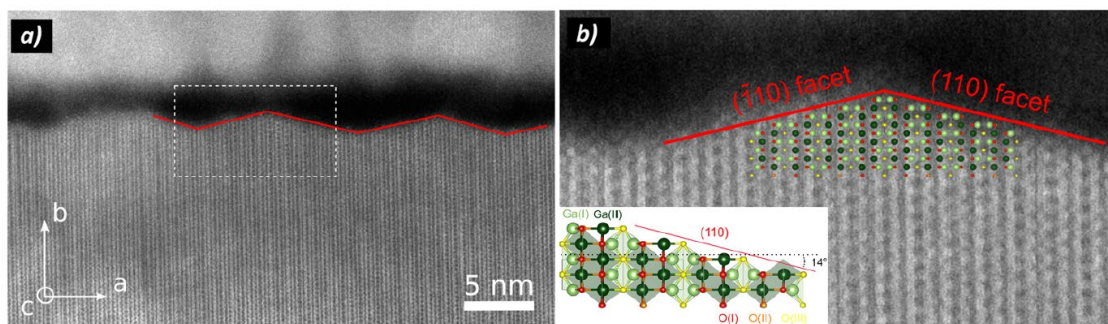


**Figure 3**. HAADF-STEM images in the c-projection of the layer (a) showing the (110) and ($\bar{1}$10) faceting on the growth surface of the sample deposited in the presence of an additional In-flux at Tg = 900 °C. (b) high-magnification image of the indicated region in (a) with an overlay of the Ga2O3 atomic model; in the image, the same ß-$Ga_2O_3$ atomic model shown in Fig. 2e is also reported as reference.

## Faceting and Step flow growth on β-$Ga_2O_3$ (100)

As shown by our etching experiments, (100) surfaces are stable under Ga-etching and oxygen annealing. We will show in the following that faceting on these surfaces has strong implications in terms of stability of surface steps with consequences on structural and electrical properties of homoepitaxial layers.[19] Due to the low effective surface diffusion coefficient of adatoms, miscut angles as high as 6 ° vs. <001> are needed to promote regular step flow growth.[12] As a consequence of the low symmetry of the monoclinic lattice, miscut direction vs. [001] and [00$\bar{1}$] are not equivalent. This is due to the fact that the plane spanned by a* and b is not a mirror plane. Fig. 4 shows AFM images of annealed surfaces and epitaxial layers on surfaces with identical miscut angle vs. these different directions. Two important findings have to be mentioned here. First, steps on surfaces with miscut towards [001] exhibit monolayer steps aligned along [010] before and after growth, while annealed substrate surfaces miscut vs. [001] exhibit a mixture of bilayer steps and monolayer steps before growth, and a surface characterized by step bunching after growth. More striking than these findings are our TEM results, which show that (i) the complete layer grown on substrates with miscut towards [001] is twinned with respect to the substrate and that the miscut at the growth surface is towards [00-1], i.e. exactly opposite to that of the substrate (cf. Fig.5).
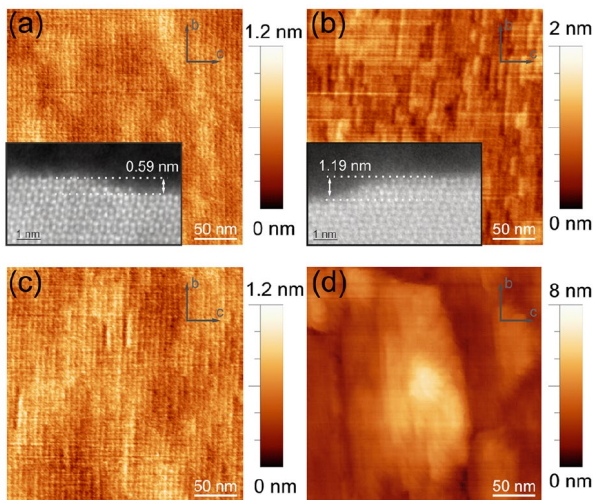
*Figure 4.* AFM images of annealed β-Ga₂O₃ (100) substrates with a miscut of 6° toward (a) the [00-1] and (b) the [001] directions. The insets show atomically resolved cross-sectional STEM images (Ga atoms appear as bright dots) recorded along the [010] projection direction, of the layer grown on the substrates shown in (a) and (b), respectively. The step in (a) is a monolayer step of half a unit cell thickness; the step in (b) is a bilayer step of a unit cell height; [(c) and (d)] AFM images of the surface of the layer grown on substrates shown in (a) and (b), respectively. Step-flow growth is observed in (c), and three-dimensional growth is observed in (d).

When analysing the atomic structure of the surface steps at the surface of layers grown with miscut along [001] and $[00\bar{1}]$ by STEM, we find that these steps are terminated by $(\bar{2}01)$ facets instead of (001) facets. The steps at the substrate surface are preserved at the interface between the twinned layer and the substrate. They are predominantly bilayer steps bound by the (001)-B facet, which according to our DFT calculations is the thermodynamically stable one. Combining our experimental findings and those from theory we can state that growth on the thermodynamically stable (100) facet is strongly affected by formation of low energy step facets. In the case of epitaxial growth on substrates with the miscut toward the $[00\bar{1}]$ direction, step edges form $(\bar{2}01)$ facets that have significantly lower surface energies than the (001) surface. If the substrate miscut is toward [001], there is no symmetry equivalent surface that would correspond to the $(\bar{2}01)$ facet. Since in this orientation all other considered surfaces are higher in energy, we would expect (001) facets to form. However, a twinned $(\bar{2}01)$ terminated nucleus forms on the (001)-B facet and converts the crystal structure into the twinned orientation directly at the step edge and thus significantly reduces the surface energy. The study of a number of samples grown under different growth conditions (e.g., growth temperature and precursor fluxes) and of various steps at the interface between the twinned layers confirms our findings. At the moment, the detailed mechanism for the nucleation as well as the detailed atomic structure of the twinned (001) facet is not fully understood since it would require a study on the oxygen atomic positions. This is however very important since twinned growth has negative impact on electrical properties.[20]
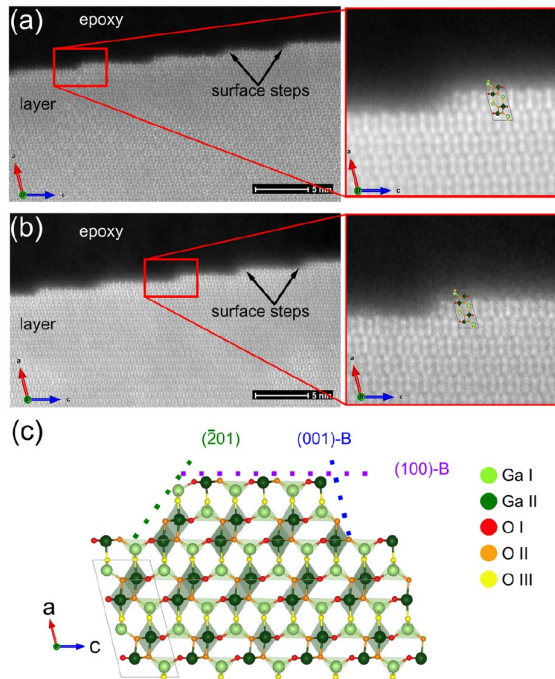
***Figure 5**. [(a) and (b)] STEM HAADF images of the surface of a layer grown on a substrate with $[00\bar{1}]$ and [001] step-down directions, respectively. The magnified regions show the typical step morphology in the [010] projection. (c) shows a stick and ball model of the observed step structure. Bright and dark green balls correspond to tetrahedrally and octahedrally bound Ga columns, respectively. Red, orange, and yellow balls correspond to the 3 different oxygen positions O(I), O(II), and O(III), respectively.*

## Conclusions and implications

Our experimental and theoretical work has shown that the differences in surface energies in β-Ga$_2$O$_3$ have strong implications on homoepitaxial growth. Faceting originates from surface energy minimization and appears to be reciprocal in case of etching and growth. In fact, a detailed study on surface energy as dependent on the chemical potential still has to be performed by both experiment and theory. Up to now, the (100) surfaces is the only one that shows the desired step flow growth. However, we have also shown that formation of low energy facets at steps and the low symmetry of the monoclinic lattice has strong implications when choosing the right miscut in β-Ga$_2$O$_3$. Unexpectedly the $(\bar{2}01)$ surface has a surface energy that is even lower than that of the second cleavage plane (001). In spite of the fact that substrates with large diameter with these orientations are available it might be worth to study growth on this surface. As in the case of the (100) surface choosing the appropriate miscut might be the key to get high quality layers.

[1]   Z. Galazka, R. Uecker, K. Irmscher, M. Albrecht, D. Klimm, M. Pietsch, M. Brützam, R. Bertram,
      S. Ganschow, and R. Fornari,
      Cryst. Res. Technol. **45**, 1229 (2010). DOI: 10.1002/crat.201000341

[2]   H. Aida, K. Nishiguchi, H. Takeda, N. Aota, K. Sunakawa, and Y. Yaguchi,
      Jpn. Appl. Phys., Part I **47**, 8506 (2008). DOI: 10.1143/jjap.47.8506

* [3]  Z. Galazka, R. Uecker, D. Klimm, K. Irmscher, M. Naumann, M. Pietsch, A. Kwasniewski, R. Bertram, S. Ganschow,
      and M. Bickermann,
      ECS J. Solid State Sci. Technol. **6**, Q3007 (2017). DOI: 10.1149/2.0021702jss

[4]   G. Wagner, M. Baldini, D. Gogova, M. Schmidbauer, R. Schewski, M. Albrecht, Z. Galazka, D. Klimm, and R. Fornari,
      Phys. Status Solidi A **211**, 27 (2014). DOI: 10.1002/pssa.201330092

* [5]  M. Baldini, M. Albrecht, A. Fiedler, K. Irmscher, D. Klimm, R. Schewski, and G. Wagner,
      J. Mater. Sci. **51**, 3650 (2016). DOI: 10.1007/s10853-015-9693-6

* [6]  M. Baldini, M. Albrecht, A. Fiedler, K. Irmscher, R. Schewski, and G. Wagner,
      ECS J. Solid State Sci. Technol. **6**, Q3040 (2017). DOI: 10.1149/2.0081702jss

[7]   T. Oshima, N. Arai, N. Suzuki, S. Ohira, and S. Fujita,
      Thin Solid Films **516**, 5768 (2008). DOI: 10.1016/j.tsf.2007.10.045

[8]   M.-Y. Tsai, O. Bierwagen, M. E. White, and J. S. Speck,
      J. Vac. Sci. Technol. A **28**, 354 (2010). DOI: 10.1116/1.3294715

[9]   K. Sasaki, M. Higashiwaki, A. Kuramata, T. Masui, and S. Yamakoshi,
      J. Cryst. Growth 378, 591 (2013). DOI: 10.1016/j.jcrysgro.2013.02.015

[10]  K. Nomura, K. Goto, R. Togashi, H. Murakami, Y. Kumagai, A. Kuramata, S. Yamakoshi, and A. Koukitu,
      J. Cryst. Growth 405, 19 (2014). DOI: 10.1016/j.jcrysgro.2014.06.051

[11]  H. Murakami, K. Nomura, K. Goto, K. Sasaki, K. Kawara, Q. T. Thieu, R. Togashi, Y. Kumagai, M. Higashiwaki,
      A. Kuramata, S. Yamakoshi, B. Monemar, and A. Koukitu,
      Appl. Phys. Express 8, 015503 (2015). DOI: 10.7567/APEX.8.015503

* [12] R. Schewski, M. Baldini, K. Irmscher, A. Fiedler, T. Markurt, B. Neuschulz, T. Remmele, T. Schulz, G. Wagner,
      Z. Galazka, and M. Albrecht, J. Appl. Phys. 120, 225308 (2016). DOI: 10.1063/1.4971957

[13]  Sasaki et al. Journal of Cryst. Growth 392, 30 (2014). DOI: 10.1016/j.jcrysgro.2014.02.002

[14]  Sang-Heon Han, et al. Semicond. Sci. Technol. 33, 045001 (2018). DOI: 10.1088/1361-6641/aaae56

[15]  S. Rafique, L. Han, A. T. Neal, S. Mou, M. J. Tadjer, R. H. French, and H. Zhao,
      Appl. Phys. Lett. 112, 052104 (2018). DOI: 10.1063/1.5017616

[16]  V. Bermudez, Chemical Physics 323, 193 (2006). DOI: 10.1016/j.chemphys.2005.08.051

[17]  G. Wulff, Zeitschrift für Krystallogr. 34, 29 (1901).

* [18] P. Mazzolini, P. Vogt, R. Schewski, C. Wouters, M. Albrecht, and O. Bierwagen,
      APL Mater. 7, 022511 (2019). DOI: 10.1063/1.5054386

* [19] R. Schewski, K. Lion, A. Fiedler, C. Wouters, A. Popp, S. V. Levchenko, T. Schulz, M. Schmidbauer, S. Bin Anooz,
      R. Grüneberg, Z. Galazka , G. Wagner, K. Irmscher , M. Scheffler, C. Draxl, and M. Albrecht,
      APL Mater. **7**, 022515 (2019). DOI: 10.1063/1.5054943

* [20] A. Fiedler, R. Schewski, M. Baldini, Z. Galazka, G. Wagner, M. Albrecht, and K. Irmscher,
      J. Appl. Phys. 122, 165701 (2017). DOI: 10.1063/1.4993748

**GraFox publications are highlighted by an "*".**